Kinetic study of pulsed desorption flows into vacuum

D. Sibold and H. M. Urbassek
Institut für Theoretische Physik, Technische Universität, D-3300 Braunschweig, Federal Republic of Germany
(Received 2 April 1990; revised manuscript received 8 February 1991)

The one-dimensional flow of particles thermally desorbed from a plane surface into vacuum is studied on the basis of a Monte Carlo simulation of the Boltzmann equation. It is assumed that particles desorb during a finite period of time with a fixed temperature. It is shown then that the flow is determined by a single parameter, which is essentially the number of monolayers Θ desorbed, and is inverse to the Knudsen number of the problem. The cases of negligible ($\Theta \ll 1$) and in part also of very intense ($\Theta \gg 1$) desorption fluxes can be treated analytically using collision-free flow and ideal gas dynamics, respectively. Here the simulation yields very good agreement with theory, indicating that the code can be used on a wide range of Knudsen numbers. For the gas-dynamical case, a Knudsen layer is formed by the equilibration of the flow in the vicinity of the surface; it is studied in some detail. Simulation of flows with $\Theta \lesssim 1$ shows that the particle distribution is far from thermal equilibrium everywhere in the flow, and deviates strongly from the analytically accessible cases. For stronger desorption fluxes, the flow is partially equilibrated, such that the velocity component in the direction of the flow reaches thermal equilibrium, although with a smaller temperature than the velocity component perpendicular to the flow. The time integrated velocity spectra of particles measured far away from the surface are discussed for moderate desorption fluxes. They are surprisingly well described by a thermal distribution, even though no Knudsen layer forms in this case.

I. INTRODUCTION

Pulsed desorption of particles from solid and liquid surfaces has been investigated intensely recently. Usually, information on the particle distribution at the surface, and hence on the desorption mechanism, is sought by measuring the properties of the desorbed particles at some distance from the surface, and by extrapolating the measured values towards the surface.[1–6] However, the density of desorbed particles in front of the surface may be so high that collisions among them will change the particle distribution considerably; in this case the extrapolation procedure becomes nontrivial.[7–9] We wish to present here a kinetic study of the effect of collisions on the particle distribution function.

Whereas the case of negligible gas density in front of the surface can conveniently be described as a collision-free flow, the other extreme case of very high gas density is considerably more complicated. In this case, immediately in front of the surface a so-called *Knudsen layer* forms, in which the nonequilibrium distribution at the surface—here all desorbed particles stream away from the surface—is transferred to a thermal equilibrium distribution with a mean flow velocity and a temperature which is considerably lower than the surface temperature. The properties of this Knudsen layer have been the subject of intense theoretical studies in the past.[10–16] Downstream of the Knudsen layer, the flow can adequately be described by the equations of ideal-gas dynamics, until further away the gas density becomes too small and the flow turns collision free.

The regime in between the very-low-density collision-free flow and the high-density gas-dynamic flow is the one which is of interest for most applications in desorption experiments. This regime is adequately described by the Boltzmann equation of rarefied gas dynamics. Here, however, no general analytical solution scheme is available. It is therefore adequate to use a numerical solution algorithm; we employ here a Monte Carlo simulation procedure.[17] This method has been used previously by other authors to study the steady evaporation flow into a background gas,[18] and the unsteady desorption into vacuum.[19,20] We wish to extend here these latter studies—which concentrated on the determination of the velocity and angular distribution of particles far away from the surface—and to investigate for a broad range of gas densities the spatial and temporal evolution of the desorption flux. By this more systematic investigation, and by comparing our simulation results with known analytical studies, a better understanding of the flow properties will be reached.

We present in this paper a kinetic study of the one-dimensional flow of particles desorbed during a finite time interval off a plane surface, which is held at a fixed temperature, into vacuum. After defining the model used (Sec. II), the collision-free case of vanishing gas density is treated analytically as a reference case (Sec. III A). The other extreme of high density can be treated by ideal-gas dynamics, implying that the flow reaches thermodynamic equilibrium at some distance from the surface (Sec. III B), and the Knudsen layer formed in this case is studied (Sec. III C). Finally, the temporal and spatial evolution of flows for moderate desorption fluxes are investigated, which are of most interest to actual desorption experiments (Sec. IV), and some conclusions on the velocity distributions far from the source are drawn.

 ©1991 The American Physical Society

II. MODEL

Particles desorb from a plane surface, which is at temperature T_0, between time $t=0$ and τ. Before and after this period of time no desorption takes place, while during this period the desorption flux

$$\Phi=\tfrac{1}{4}n_V v_T=n_0 v_0 \tag{1}$$

is constant. For a thermal desorption mechanism, the number density n_V depends on the surface temperature T_0 via the ideal-gas law $n_V=p_V/kT_0$, where $p_V(T_0)$ is the vapor pressure of the surface and k is Boltzmann's constant. The particle number density n_0 of the desorbed particles immediately outside the surface is $n_0=n_V/2$, since only particles streaming away from the surface contribute to the desorption flux. The mean thermal velocity in a gas of temperature T_0 is $v_T=\sqrt{8kT_0/\pi m}$, where m is the particle mass. Since the desorbed current is cosine distributed, the flow velocity of the desorbing particles in the direction normal to the surface is $v_0=v_T/2$.

The total number of particles desorbed per unit area consequently is

$$N=\Phi\tau\ , \tag{2}$$

and assuming each particle to occupy a surface area Σ_{atom}, the number of monolayers desorbed is

$$\Theta=\Phi\,\Sigma_{\text{atom}}\,\tau\ . \tag{3}$$

We shall treat the flow of desorbed particles as one dimensional. This is obviously justified for distances which are smaller than the lateral extension of the desorption area on the surface.

A. Boltzmann equation

We introduce a Cartesian coordinate system with its x axis in the direction of the outward surface normal and identify the surface as $x=0$. The properties of the desorbed gas particles are described by the phase-space density $f(x,\mathbf{v},t)$, which is defined such that $f(x,\mathbf{v},t)dx\,d^3v$ is the mean number of particles found at time t in an infinitesimal interval dx around the distance x from the surface and having their velocity in an infinitesimal velocity volume d^3v around $\mathbf{v}$.

We assume that the phase-space density obeys the Boltzmann equation[21,22]

$$\frac{\partial}{\partial t}f(x,\mathbf{v},t)+v_x\frac{\partial}{\partial x}f(x,\mathbf{v},t) = \int d^3v_1\int d^2\Omega\,\sigma(g,\Omega)g[f(x,\mathbf{v}_1',t)f(x,\mathbf{v}',t) - f(x,\mathbf{v}_1,t)f(x,\mathbf{v},t)]\ . \tag{4}$$

Here $g=|\mathbf{v}-\mathbf{v}_1|$ is the relative speed between two particles of velocity $\mathbf{v}$ and $\mathbf{v}_1$; $\sigma(g,\Omega)d^2\Omega$ is the scattering cross section for two particles of relative speed g to scatter into a solid angle in the center-of-mass system within an interval $d^2\Omega$ around Ω; and $\mathbf{v}_1'$ and $\mathbf{v}'$ are the velocities of two particles which after colliding with a center-of-mass angle Ω attain velocities $\mathbf{v}_1$ and $\mathbf{v}$.

We now have to specify the boundary condition at the surface. Here we assume that particles leave the surface in thermal equilibrium with it; that is, every velocity component obeys a Maxwellian distribution with temperature T_0, with the obvious but notable exception that particles must leave the surface in the outward direction, i.e., $v_x>0$:

$$f(x=0,\mathbf{v},t)=\frac{\Phi}{2\pi}\left[\frac{m}{kT_0}\right]^2\exp\left[-\frac{m\mathbf{v}^2}{2kT_0}\right], \qquad v_x>0,\quad 0<t<\tau\ . \tag{5}$$

At $t<0$ and $t>\tau$, we assume $f(x=0,v_x>0,t)\equiv 0$. The coefficient in Eq. (5) has been chosen such that the desorbed flux $\int d^3v\,v_x f\Theta(v_x)$ equals Φ; $\Theta(v_x)$ denotes Heaviside's step function. We assume desorption to proceed in vacuum. Thus our second boundary condition reads

$$f(x\to\infty,\mathbf{v},t)\equiv 0\ . \tag{6}$$

We shall adopt in the following hard-sphere interaction with a cross section

$$\sigma(g,\Omega)d^2\Omega=\frac{1}{4\pi}\Sigma d^2\Omega\ , \tag{7}$$

such that Σ is the velocity-independent total scattering cross section.

B. Scaling properties

We now wish to show that the solution of our problem depends on only one parameter, which may be expressed in terms of the number of monolayers desorbed or of the Knudsen number. To this end we scale time to τ, velocities to v_0, the distance x from the surface to

$$x_0=v_0\tau\ , \tag{8}$$

and the distribution function to $\Phi/v_0^4=n_0 v_0^{-3}$. Denoting scaled quantities by a tilde, the Boltzmann equation then reads for hard-sphere interaction (7) in an obvious and customary notation

$$\frac{\partial\tilde f}{\partial\tilde t}+\tilde v_x\frac{\partial\tilde f}{\partial\tilde x}=Z\int d^3\tilde v_1\int\frac{d^2\Omega}{4\pi}\tilde g(\tilde f_1'\tilde f'-\tilde f_1\tilde f)\ , \tag{9}$$

with the surface boundary condition

$$\tilde f(\tilde x=0,\tilde{\mathbf{v}},\tilde t)=\frac{2}{\pi^3}e^{-\tilde{\mathbf{v}}^2/\pi},\quad \tilde v_x>0 \tag{10}$$

for $0<\tilde t<1$, and zero otherwise.

The parameter Z is given by

$$Z=\Phi\Sigma\tau\ . \tag{11}$$

This parameter determines all physical quantities characterizing the system. It is immediately related to the number Θ of monolayers desorbed, Eq. (3), if we note that the area Σ_{atom} an atom occupies at the surface is roughly $\frac{1}{4}$ of the gas-kinetic cross section Σ, and hence

$$Z \cong 4\Theta \ . \tag{12}$$

Z is as well connected to the Knudsen number Kn of the system, albeit in an indirect way, since this depends on the—*a priori* unknown—form of the particle distribution function at the surface. The Knudsen number is defined as the ratio of the mean free path λ near the surface to the typical length scale x_0 of the problem

$$\mathrm{Kn} = \frac{\lambda}{x_0} \ . \tag{13}$$

The mean free path depends on the particle distribution at the surface. Assuming for the sake of simplicity the gas to be in thermal equilibrium, for a hard-sphere gas it is

$$\lambda = \frac{1}{\sqrt{2}\Sigma n_0} \ , \tag{14}$$

and hence

$$\mathrm{Kn} = \frac{1}{\sqrt{2}Z} \ . \tag{15}$$

Alternatively, Kn may be calculated for a half-Maxwellian distribution at the surface, Eq. (5), i.e., disregarding backscattered particles; this gives a result very similar to Eq. (15).

C. Simulation

An analytical solution scheme of the Boltzmann equation (4) with the boundary condition (5) is not available. We therefore solved the problem via a Monte Carlo computer simulation. We adopted Bird's algorithm,[23,17] which roughly proceeds as follows: Space is divided into cells, which are chosen here as plane slabs parallel to the surface. For small Z, 100 cells, and for larger Z up to 2500 cells were used. Within each cell particles may collide; collision partners are chosen in a Monte Carlo procedure based on the statistics of the collision frequencies of the particle pairs available. After a time step Δt every particle is moved a distance $\mathbf{v}\Delta t$ according to its individual velocity $\mathbf{v}$, and may leave its cell. Then the collision procedure restarts, etc. If a particle hits the surface or leaves the outermost cell, it is absorbed.

According to this algorithm, the particle distribution evolves in time. We start at time $t=0$ when all cells are empty, and let particles desorb from the surface according to the half-Maxwellian distribution (5) until time $t=\tau$. We sample the distribution in all cells at predetermined times. This procedure is repeated several, typically 20, times, until sufficient statistics has accumulated. Table I summarizes important technical parameters of the simulation. For further details of the algorithm the reader is referred to Refs. 17 and 24. We note that the algorithm gives poor results when too few particles are in a cell. This happens in the expansion front far away from the surface. In the figures below, we therefore present results only when the number of particles in a cell is larger than 5.

TABLE I. Important parameters of simulations.

Z	Number of cells	Cell width $\Delta x/x_0$	Time step $\Delta t/\tau$	Total number of particles	Number of runs
1	100	0.18	0.1	20 000	150
10	500	3.5×10^{-2}	2.0×10^{-2}	50 000	103
100	2500	7.1×10^{-3}	3.3×10^{-3}	50 000	25

III. SOLUTION FOR VERY SMALL AND VERY LARGE DESORPTION FLUXES

In the case of very intense desorption, $Z \gg 1$, the collision frequency is very large, such that the particle distribution is locally in equilibrium and gas dynamics applies. In the reverse case of very weak desorption fluxes, $Z \ll 1$, collisions can be ignored, and the distribution approaches that of a collision-free flow. The latter case can be treated completely analytically, the first case to a large part. It is instructive to discuss shortly these solutions, since they represent the extreme cases of desorption flows, between which the analytically inaccessible regime of $Z \simeq 1$ is situated, which we shall study in the next section. These cases also allow to test our algorithm. In Sec. III C we shall furthermore study some properties of the Knudsen layer which is present for intense desorption fluxes.

The information present in the distribution function $f(x,\mathbf{v},t)$ is far too detailed to be of immediate use. In this section we shall restrict our attention to the following four moments of the distribution:

$$\begin{aligned} n(x,t) &= \int d^3v\, f(x,\mathbf{v},t) \ , \\ u(x,t) &= \frac{1}{n}\int d^3v\, v_x f(x,\mathbf{v},t) \ , \\ T_{\parallel}(x,t) &= \frac{1}{n}\frac{m}{k}\int d^3v (v_x-u)^2 f(x,\mathbf{v},t) \ , \\ T_{\perp}(x,t) &= \frac{1}{2n}\frac{m}{k}\int d^3v (v_y^2+v_z^2) f(x,\mathbf{v},t) \ , \end{aligned} \tag{16}$$

which describe the spatial and temporal dependence of the number density n, the flow velocity u, and the variances of the distribution in the direction parallel and perpendicular to the flow, $T_{\parallel}$ and $T_{\perp}$. Following customary notation these have been expressed as temperatures. It is obvious that a temperature proper only exists, if not only each velocity component is equilibrated, but if $T_{\parallel}$ and $T_{\perp}$ coincide. It is sometimes useful to introduce at least formally a (mean) temperature T as

$$T = \tfrac{1}{3}(T_{\parallel} + 2T_{\perp}) \ . \tag{17}$$

A. Collision-free flow

For very moderate desorption fluxes, it is $Z \to 0$ and we may ignore the influence of collisions altogether. Thus the right-hand side of Eq. (9) vanishes, and the distribution function f and its moments may easily be obtained analytically (cf. Appendix A). We display the moments in graphical form in Fig. 1, and note the following.

(i) At $t<\tau$, the density has its maximum $n=n_0$ at the surface, where the flow velocity is $u=v_0$. The density diminishes farther away from the surface, since there only

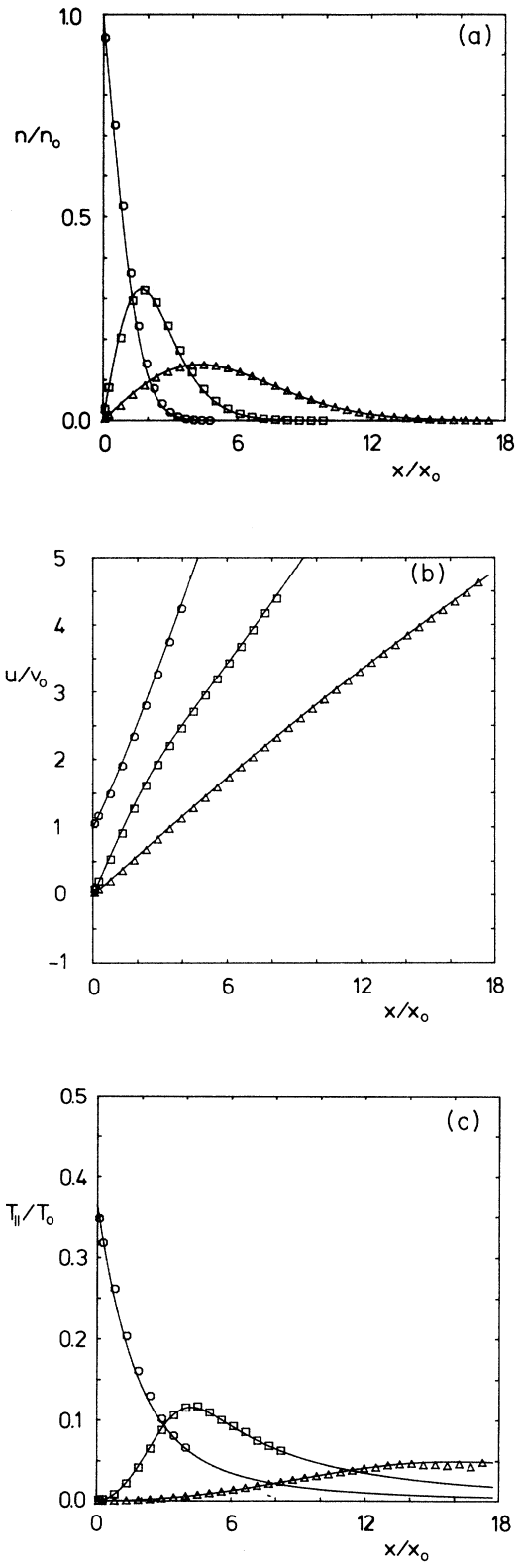

FIG. 1. (a) Number density n, (b) flow velocity u, and (c) temperature in flow direction $T_{\parallel}$ as a function of the distance x from the surface at time $t=\tau$ (○), $t=2\tau$ (□), and $t=4\tau$ (△). Collision-free flow $Z=0$. Symbols denote simulation results, lines the analytical solution (A5).

the fastest particles of the tails of the source Maxwellian are found. Correspondingly, the flow velocity increases away from the surface, while the pertinent temperature, i.e., the variance of the velocity distribution in flow direction, decreases.

(ii) At $t>\tau$, a gas cloud forms, which moves away from the surface with time, and disperses. The density immediately at $x=0$ is zero, since no particles are desorbed anymore, while—due to the lack of collisions—no particles can be scattered back towards the surface. Likewise the flow velocity vanishes here, since all particles which remain close to the surface must have zero velocity. Particles at large distances x must obey $v\cong x/t$, since they traveled a distance x in roughly time t. According to this argument, at large x, the temperature in the direction of the flow $T_{\parallel}$ must be small and the flow velocity $u=x/t$.

(iii) Due to the lack of collisions, the distribution is in nonequilibrium, $T_{\parallel}\neq T_{\perp}$ everywhere.

(iv) Since the desorption conditions do not change along the surface, v_y and v_z obey a Maxwellian distribution everywhere with $T_{\perp}=T_0$.

As exemplified in Fig. 1, our simulation is in good agreement with the analytical results.

B. Gas dynamics

The case of very large desorption fluxes $Z\gg 1$ is considerably more intricate. Here the flow can evidently be divided into three regimes.

(i) The Knudsen layer adjacent to the surface, where the nonequilibrium distribution immediately at the surface $x=0$ changes due to collisions and reaches equilibrium at a distance x_K from the surface.

(ii) A region in which there are sufficient collisions to couple all degrees of freedom, such that it can be described by ideal-gas dynamics.

(iii) Farther away the density is too low to keep the distribution in equilibrium, and the flow changes gradually to a collision-free flow.

In this paper we shall not investigate regime (iii), since here our restriction to a one-dimensional geometry may be too severe. We shall discuss the gas-dynamic regime (ii) in this subsection and the Knudsen layer (i) in Sec. III C.

In order to determine the gas-dynamic solution for region (ii), the pertinent boundary conditions must be given. It is known from analytical considerations that at the end of the Knudsen layer the flow attains sound speed.[12,15] It is shown in Appendix B that then for times $t<\tau$ the gas-dynamic solution can be written down as a so-called centered wave:

$$n(x,t)=n_K\left[\frac{T}{T_K}\right]^{3/2},$$

$$u(x,t)=u_K+\frac{3}{4}\frac{x-x_K}{t},\quad t<\tau,\quad 0<x-x_K<4u_K t, \tag{18}$$

$$T(x,t)=\frac{3}{5}\frac{m}{k}\left[u_K-\frac{1}{4}\frac{x-x_K}{t}\right]^2,$$

TABLE II. Gas density n, flow velocity u, temperature T, current $j=nu$, and Mach number M at the end of the Knudsen layer $x=x_K$: Comparison between simulation results for $Z=100$ and analytical theory (after Ref. 12).

Method	n_K/n_0	u_K/v_0	T_K/T_0	j_K/Φ	M_K
Simulation	0.64±0.03	1.29±0.04	0.65±0.02	0.83±0.04	0.99±0.03
Theory	0.62	1.31	0.65	0.82	1

where we assumed a monoatomic gas, $u_K=\sqrt{\frac{5}{3}(kT_K/m)}$ is the constant flow speed at the end of the Knudsen layer x_K, and T_K and n_K are the constant temperature and density there. In order to compare this solution with our simulation results, the values of these constants must be determined from a consideration of the location and the flow properties at the end of the Knudsen layer, as will be discussed in Sec. III C (cf. also Table II). We are working on obtaining a complete analytical solution of the gas-dynamic expansion for $t>\tau$,[25] cf. also Ref. 26.

In Fig. 2, we plot the gas-dynamic solution and compare it with the simulation results of $Z=100$, corresponding to a Knudsen number of $\mathrm{Kn}\cong 0.007$. At $t=\tau$ good agreement between the gas-dynamic results and the simulation data is achieved. Immediately at the surface, in the Knudsen layer, gas dynamics does not hold (see below). For $x>3.5x_0$, we furthermore observe an increase in the temperature which is due to a lack of equilibration in the front of the expansion wave. As an analysis of the data shows, in particular the temperature perpendicular to the flow direction $T_\perp$ increases considerably in this region (cf. also Fig. 5 below).

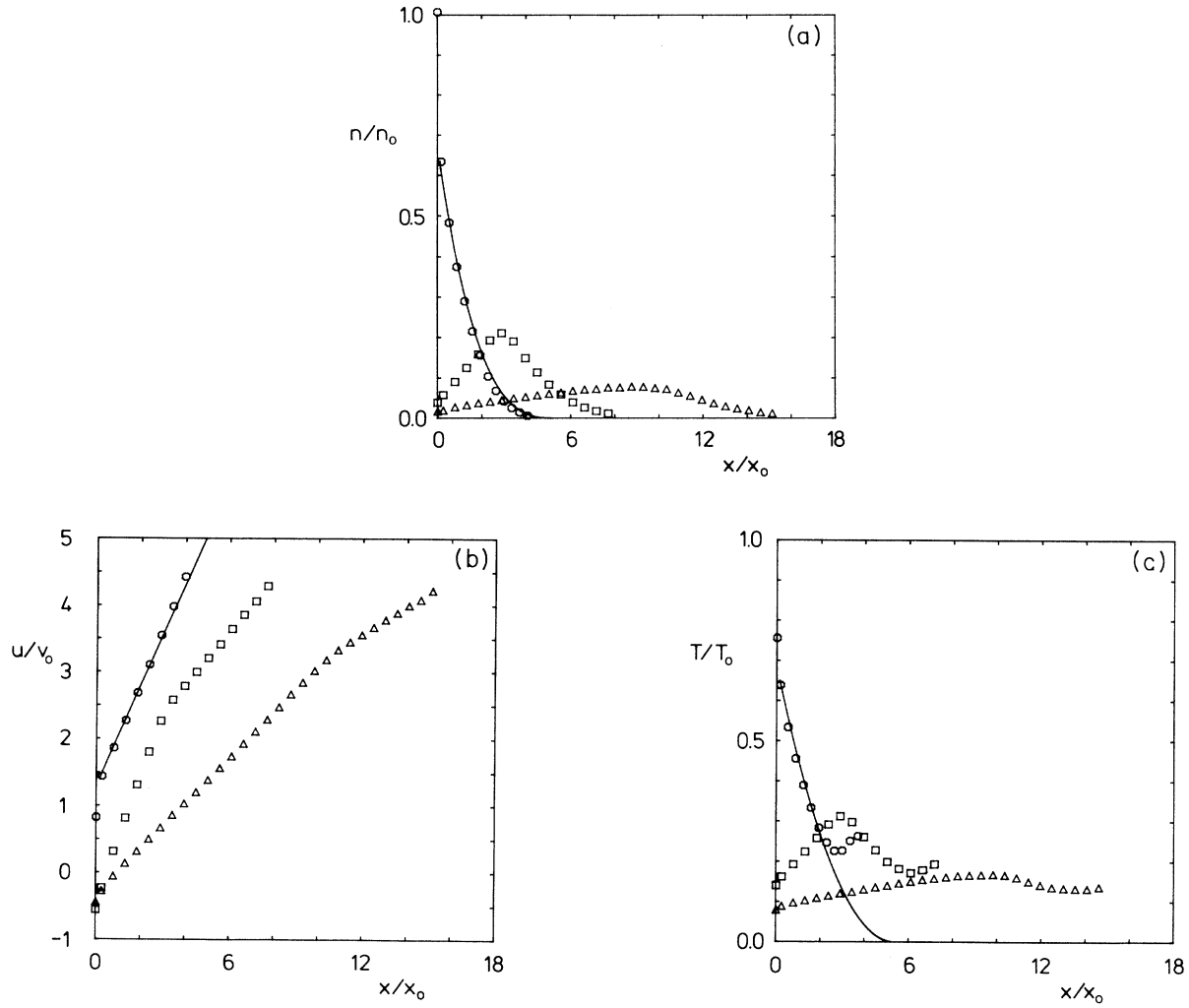

FIG. 2. (a) Number density n, (b) flow velocity u, and (c) temperature T as a function of the distance x from the surface at time $t=\tau$ (○), $t=2\tau$ (□), and $t=4\tau$ (△). Symbols, simulation results for $Z=100$. Line, gas-dynamic solution for $t=\tau$.

At later times, it is seen how the expansion wave gets separated from the surface and streams into vacuum, while a low-density region exists between the surface and the end of the simple expansion wave. In particular, at $t=2\tau$, a rather sharp change in slope of $u(x,t=2\tau)$ is observed at the place where these two regions meet, i.e., at the maximum of the density $n(x,t=2\tau)$. At this place, the temperature has its maximum also: In the expansion wave, thermal energy is transformed to kinetic flow energy, and hence temperature decreases in the direction away from the surface. Going from the density maximum towards the surface, temperature must also decrease, since it is only low-energy particles which are left in this region, and since the surface absorbs particles, and hence energy. While Fig. 2 shows results which appear qualitatively quite similar to the collision-free solution of Fig. 1, we wish to direct the attention to two changes. First the gas cloud travels faster and disperses more quickly than in the collision-free case; this is evidently due to the pressure gradient acting as an additional driving force on the wave. Secondly, at $t>\tau$, density and flow velocity immediately at the surface do not vanish in the gas-dynamic case. This is due to particles scattered back from the gas cloud towards the surface. In particular, the gas cloud does not separate from the surface. Negative velocities occur because we adopted the boundary condition that every particle impinging on the wall $x=0$ sticks there; this simulates recondensation at the wall. These features are now discussed more quantitatively by a consideration of the Knudsen layer.

C. Knudsen layer

The flow field immediately at the surface cannot be described by gas dynamics. This is due to the strong thermodynamic nonequilibrium which is imposed by the boundary condition at the surface itself, which assumes all desorbed particles to have velocities $v_x>0$. Here a kinetic study is mandatory. Such a study is possible by our simulation scheme. We present in Fig. 3 the results of a simulation with $Z=100$ at $t=\tau$ for the temperature and the Mach number ($M=u/c$, where c is the local velocity of sound) close to the surface, and in Fig. 4 the velocity distribution in flow direction

$$F(x,v_x,t)=\int dv_y dv_z f(x,\mathbf{v},t)\Big/\int d^3v\, f(x,\mathbf{v},t)\ . \qquad (19)$$

The following observations can be made.

(i) As is observed in Fig. 2, the surface density is almost equal to the collision-free case [$n(x=0)=1.01n_0$], whereas the flow velocity is considerably reduced [$u(x=0)=0.82v_0$]. Due to backscattering hence the net desorption flux is reduced to a value of $j(x=0)=0.83\Phi$. This value is in good agreement with the analytical estimate for the steady state,[12] cf. Table II. We note that, strictly speaking, the simulation data given here are valid as an average on a surface region extending from $x=0$ to $x=0.018x_0$.

(ii) The temperatures in flow direction $T_\parallel$ and perpendicular to it $T_\perp$ roughly coincide at $x=0.13x_0$. The velocity distribution in the flow direction has been sampled at $x=0.03x_0$. It may well be fitted by a shifted Maxwellian

$$F(x,v_x,t)=\left[\frac{m}{2\pi kT}\right]^{3/2}\exp\left[-\frac{m(v_x-u)^2}{2kT}\right], \qquad (20)$$

indicating that at this point the distribution has equilibrated thermally in flow direction via collisions.

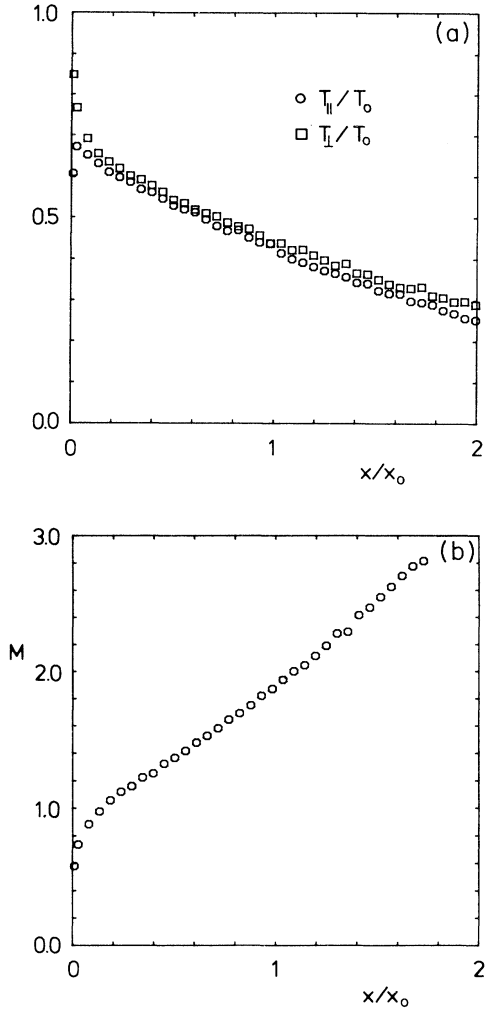

FIG. 3. Temperature in flow direction $T_\parallel$ (○) and perpendicular to it $T_\perp$ (□) (a) and Mach number M (b) as a function of the distance x from the surface at time $t=\tau$. Simulation results for $Z=100$.

(iii) The Knudsen layer has a width of $x_K\cong 0.13x_0$. Given $\mathrm{Kn}\cong 0.007$, this amounts to an extension over 19λ. It is difficult to estimate the width of the Knudsen layer analytically, but it is expected to extend over "a few mean free paths,"[11,12,15] in agreement with our simulation result.

(iv) The flow is subsonic in the Knudsen layer and supersonic in the gas-dynamic outer layer. It transits $M=1$ at $x\simeq 0.15x_0$, which roughly is the end of the Knudsen

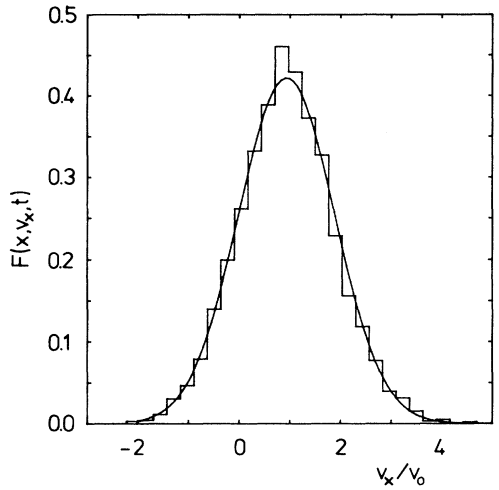

FIG. 4. Velocity distribution in flow direction $F(x,v_x,t)$ at $t=\tau$ and $x=0.03x_0$. Histogram, simulation result for $Z=100$. Line, fit to a shifted Maxwellian, Eq. (20). Fit parameters: $u=0.94v_0$, $T=0.57T_0$.

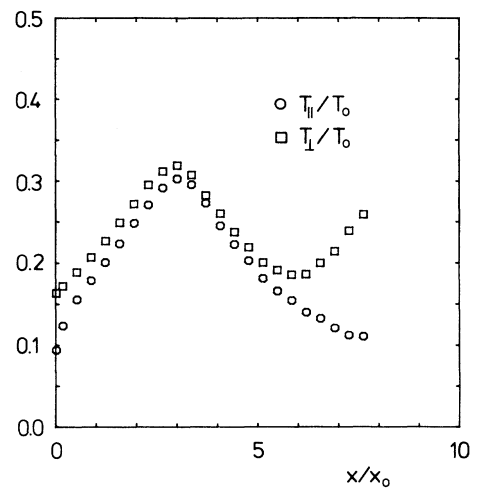

FIG. 5. Temperature in flow direction $T_\parallel$ (○) and perpendicular to it $T_\perp$ (□) as a function of the distance x from the surface at time $t=2\tau$. Simulation results for $Z=100$.

layer $x_K \cong 0.13x_0$. This is in agreement with theoretical considerations which argue that the entropy production which accompanies the equilibration of the flow in the Knudsen layer allows the flow to exceed the velocity of sound. In the equilibrated gas-dynamic regime the flow is supersonic.[12,15]

(v) We compare in the table the results of our simulations for various quantities at the end of the Knudsen layer with analytical estimates. Good agreement is obtained. This shows that after $t=\tau$ a Knudsen layer has formed which is well described by the analytical theory of stationary flows.

Analytic treatments of the Knudsen layer[11–13,15,16] suffer from a number of drawbacks: They have difficulties in predicting the extension of the Knudsen layer, and they have to make assumptions on the form of the distribution function of backscattered particles at the surface. It is therefore necessary to supplement these analytic efforts with detailed *ab initio* kinetic studies. Simulations like the one presented here are able to perform such investigations.

We finally wish to note that after the end of the desorption process $t>\tau$, the Knudsen layer tends to become destroyed again due to the small particle densities in the vicinity of the surface. Figure 5 exemplifies this fact by displaying the temperatures in flow direction and perpendicular to it at $t=2\tau$. While in the region $3x_0<x<5x_0$, which constitutes the regime of the expansion wave separated from the surface, thermal equilibrium is still conserved, the flow is in nonequilibrium at $0<x<x_0$. Close to the expansion front, $x \gtrsim 6x_0$, the flow could not equilibrate due to too small particle densities.

IV. SOLUTION IN THE KINETIC REGIME $Z \cong 1$

For values of the parameter Z around 1—and hence for desorption fluxes in the experimentally interesting regime $\Theta \cong 1$—collisions do affect the particle distribution, such that the results obtained for collision-free flows do not hold; on the other side, the number of collisions is still small, such that local thermodynamic equilibrium is not established and the gas-dynamic equations do not yet describe the flow. This makes a kinetic description of the flow mandatory. In the following we shall analyze such a flow with the help of computer simulation results.

A. Moderate desorption

We display in Fig. 6 the moments of the simulation solution for the case of moderate desorption $Z=1$, for which around $\Theta=0.25$ monolayers are desorbed, Eq. (3). It is seen that at the end of the desorption period $t=\tau$, density and flow velocity are sufficiently well described as a collision-free flow, whereas the temperatures show that collisions lead to an energy flow from the velocity component perpendicular to the flow into the flow direction. This effect becomes more and more substantial with increasing time, such that at $t=4\tau$ around 70% of the transverse energy is put into kinetic energy of motion in the flow direction; most of this energy becomes thermal energy, while the flow velocity is only marginally influenced around the density maximum. Close to the surface, however, a considerable backflow of desorbed particles towards the surface is established, as evidenced by the nonvanishing density at the surface and the negative flow velocity there.

Evidently, the flow is nowhere in thermal equilibrium, since the two component temperatures nowhere coincide. In Fig. 7 we plot the velocity distribution in the flow direction in two example cases: close to the surface at $t=\tau$, and at the density maximum at $t=2\tau$. It is observed that this partial distribution is nowhere in equilibrium in itself, although in the latter example, it appears to be not too badly described by a shifted Maxwellian dis-

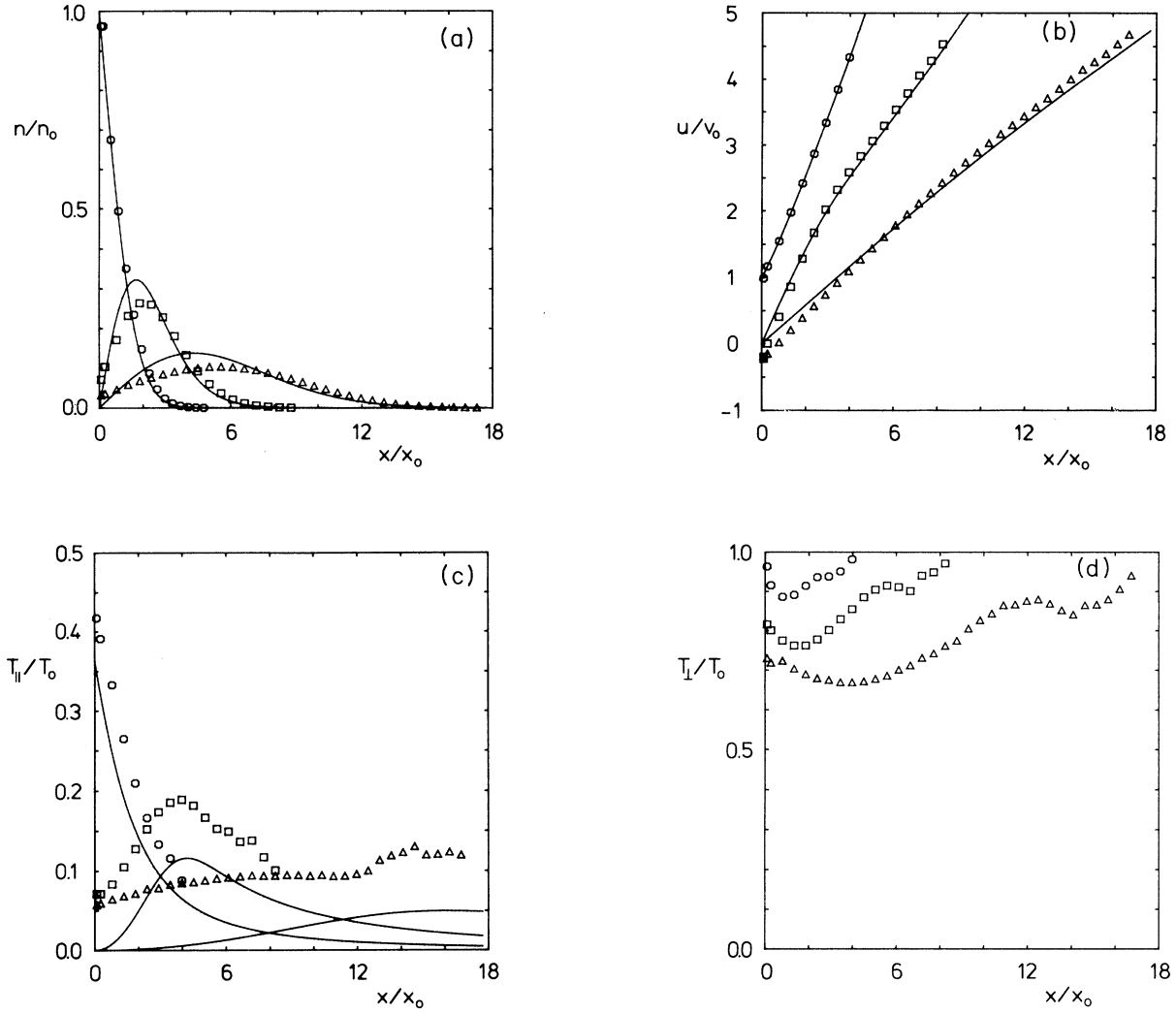

FIG. 6. (a) Number density n, (b) flow velocity u, (c) temperature in flow direction $T_{\parallel}$, and (d) perpendicular to it $T_{\perp}$ as a function of the distance x from the surface at time $t=\tau$ (○), $t=2\tau$ (□), and $t=4\tau$ (△). Symbols denote simulation results for $Z=1$, lines the analytical results for a collision-free flow Eq. (A5).

tribution (20). Of course, the velocity component perpendicular to the flow is in much better equilibrium in itself (not shown here).

B. Intense desorption

An example of more intense desorption ($Z=10$), equivalent to $\Theta=2.5$ monolayers desorbed, is displayed in Fig. 8. We omitted the results for the density and flow velocity distribution, since the influence of collisions on these distributions has already been discussed at length. As evidenced in Fig. 8, the temperature components parallel and perpendicular to the flow direction nowhere coincide even for such an intense desorption flux. The velocity distribution in Fig. 9, however, shows that each velocity component is in itself quite well equilibrated. We therefore expect that this desorption flow might well be described in terms of a so-called ellipsoidal distribution function with two temperatures.

C. Velocity spectra at large distances

A typical experimental procedure for observing the properties of desorbed particles is to measure the velocity distribution of particles flying into a definite angle far away from the source, where collisions cease. Typical detectors measure the *flux* of particles streaming into direction $\mathbf{\Omega}$

$$\mathbf{v}f(x,\mathbf{v},t)d^3v=\mathbf{\Omega}v^3f(x,v,\mathbf{\Omega},t)dv\,d^2\Omega\ . \tag{21}$$

The velocity spectrum of particles hitting at any time t a detector, which is oriented perpendicular to the flow direction $\mathbf{\Omega}$ at a distance x_D from the surface, is then given by

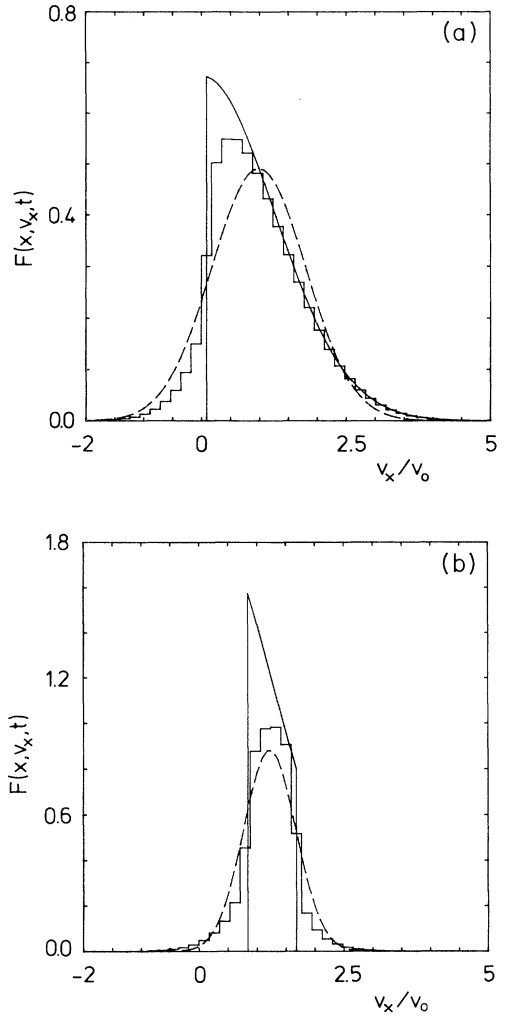

FIG. 7. (a) Velocity distribution in flow direction $F(x,v_x,t)$ close to the surface $x=0.09x_0$ at $t=\tau$ and (b) at a later time $t=2\tau$ at the density maximum $x=1.7x_0$. Histogram, simulation result for $Z=1$. Solid line, analytical result for collision-free flow, Eq. (A5). Dashed line, fit to a shifted Maxwellian, Eq. (20). Fit parameters: (a) $u=0.99v_0$, $T=0.42T_0$; (b) $u=1.22v_0$, $T=0.13T_0$.

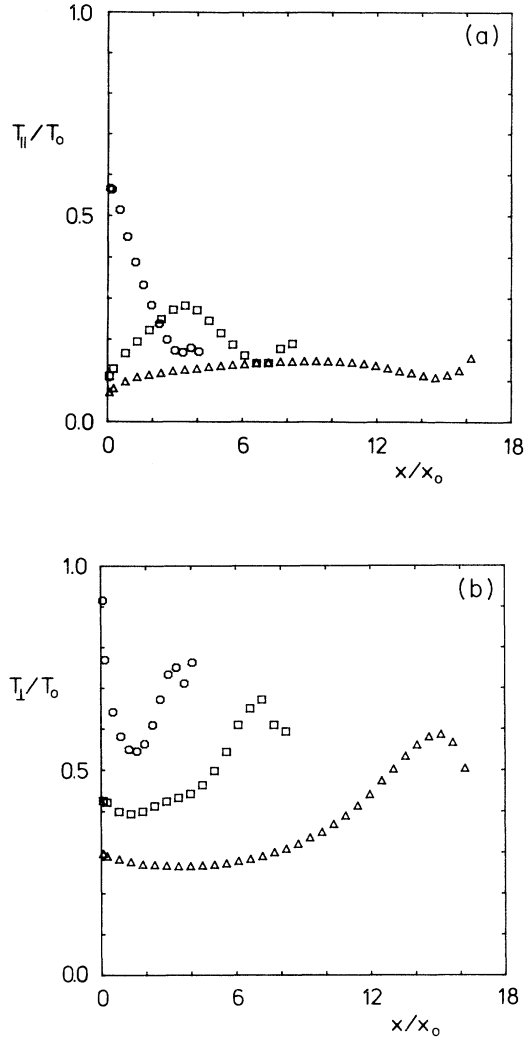

FIG. 8. (a) Temperature in flow direction $T_\parallel$ and (b) perpendicular to it $T_\perp$ as a function of the distance x from the surface at a time $t=\tau$ (○), $t=2\tau$ (□), and $t=4\tau$ (△). Simulation results for $Z=10$.

$$\int_0^\infty dt\, v^3 f(x_D,v,\Omega,t)\ . \tag{22}$$

Far away from the surface, where collisions cease, the form of the spectrum will be independent of x_D. We denote by ϑ the polar angle of the velocity direction Ω towards the surface normal, and by φ its azimuth. Integrating over the uninteresting azimuthal angle, and normalizing, we finally obtain

$$J(v,\vartheta)=\int_0^\infty dt \int_0^{2\pi} d\varphi\, v^3 f(x_D,v,\Omega,t) \Big/ \int_0^\infty dv \int_0^\infty dt \int_0^{2\pi} d\varphi\, v^3 f(x_D,v,\Omega,t)\ . \tag{23}$$

Our one-dimensional description only works for small or moderate desorption intensities, because otherwise the effects of collisions will be sensible at distances from the surface which are larger than the width of the desorption spot on the surface. In Fig. 10 we display velocity spectra simulated for $Z=1$, corresponding to the desorption of $\Theta=0.25$ monolayers. In this case, the detector distance in the simulation was chosen as $x_D=35x_0$, and the

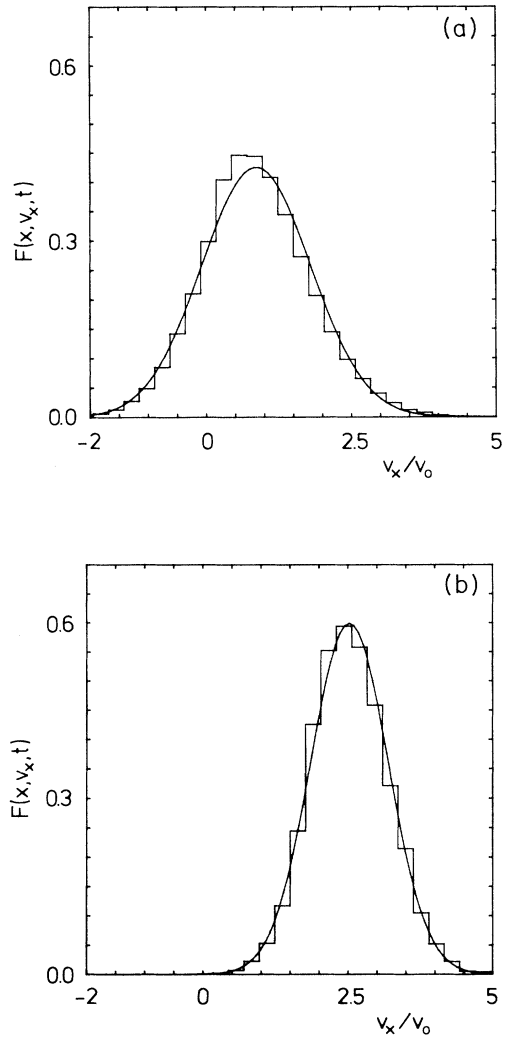

FIG. 9. (a) Velocity distribution in flow direction $F(x,v_x,t)$ close to the surface $x=0.05x_0$ at $t=\tau$ and (b) at a later time $t=2\tau$ at the density maximum $x=3.5x_0$. Histogram, simulation result for $Z=10$. Line, fit to a shifted Maxwellian, Eq. (20). Fit parameters: (a) $u=0.87v_0$, $T=0.56T_0$; (b) $u=2.53v_0$, $T=0.28T_0$.

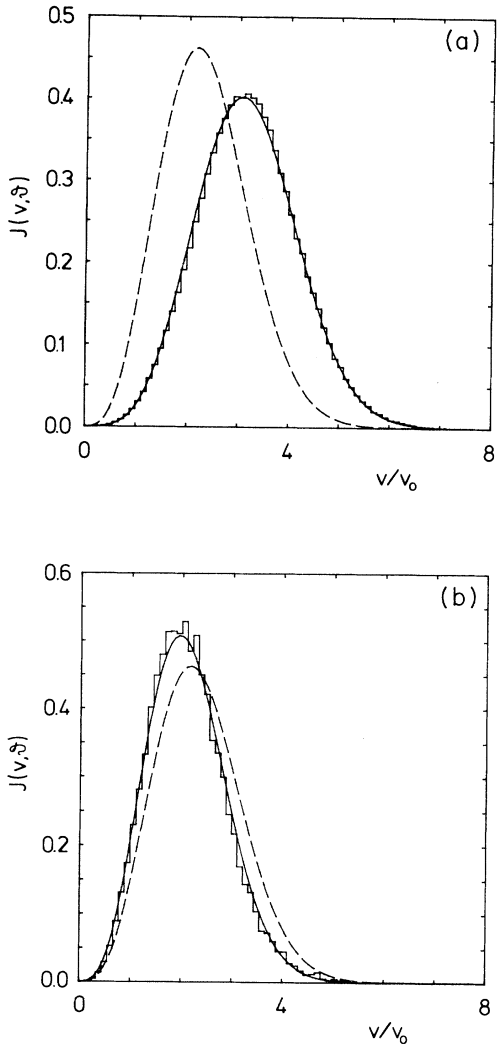

FIG. 10. Velocity spectra $J(v,\vartheta)$ far from the surface for particles flying into an angle of (a) $\vartheta=0°$ and (b) $\vartheta=60°$ from the surface normal. Histogram, simulation result for $Z=1$. Dashed line, analytical result for collision-free flow, Eq. (A8). Solid line, fit to a shifted Maxwellian, Eq. (24). Fit parameters: (a) $u=1.58v_0$, $T=0.97T_0$; (b) $u=-0.09v_0$, $T=0.85T_0$.

maximum detection time as 500τ. It is observed that the energy spectra can well be fitted to the flux of a steady thermal source

$$J(v,\vartheta)\propto v^3\exp\left[-\frac{m(v-u)^2}{2kT}\right], \tag{24}$$

and that the fitted temperature is—for perpendicular emission $\vartheta=0°$—in quite good agreement with the surface temperature. It is quite remarkable that this fit is possible, since we saw in Sec. III B that this flow is nowhere in thermodynamic equilibrium. However, already in a previous investigation, it was observed that the time integrated distribution function far away from the surface can be described as an ellipsoidal distribution, even for relatively few collisions per particle.[27] This implies that the flux J should obey a shifted Maxwellian distribution, Eq. (24).

We observe that energetic particles fly predominantly in the direction perpendicular to the surface rather than at oblique angles. This fact has been mentioned previously in Refs. 1, 19, and 20. It is due to a simple kinematic effect: When two particles collide, after the collision the faster particle will be closer to the center-of-mass velocity. Since this is on the average in the direction of the surface normal, after a few collisions faster particles are found predominantly in this direction. In terms of the macroscopic moments (16), this phenomenon corresponds to an energy flow from the velocity component perpendicular to the flow into the flow direction, which

increases u and in particular $T_\parallel$ at the cost of $T_\perp$ (cf. Sec. IV A and Fig. 6).

V. CONCLUSION

We studied the one-dimensional flow of particles desorbed thermally during a finite period of time into vacuum. It was shown that this problem depends on only one parameter, which is essentially the number of monolayers desorbed and is the inverse of the Knudsen number of the problem. The flow was investigated by a Monte Carlo simulation of the Boltzmann equation.

Comparison with analytical results for collision-free flows at negligible desorption fluxes, and for gas-dynamic flows at intense desorption fluxes gives good agreement with our simulation results. In the latter case we study the Knudsen layer formed close to the surface and show that it agrees with the analytical description of stationary Knudsen layers. A particular result, which can hardly be obtained by other methods, is the width of the Knudsen layer for a flow of Kn=0.007, which amounts to 19 free mean paths.

Flows originating from the desorption of less than around 1 monolayer nowhere attain thermal equilibrium and hence are not describable by gas dynamics. On the other side, collisions lead to a definite backflow of desorbed particles towards the surface, and to an increase of the velocity in the direction of the flow. Hence the flow characteristics deviate as well from those of a collision-free flow. Velocity spectra taken far away from the surface may surprisingly well be fitted by a shifted Maxwellian, with a temperature close to the surface temperature.

With the desorption of more than around one monolayer, the velocity distribution of the flow reaches thermodynamic equilibrium in each velocity component itself, i.e., the velocity component parallel to the flow is well described by a shifted Maxwellian distribution. However, the temperatures parallel and perpendicular to the flow do not coincide, such that a gas-dynamic analysis does not apply before around 10 monolayers are desorbed. In that case, a three-dimensional description of the jet ought to be undertaken, which is outside the scope of the present investigation.

ACKNOWLEDGMENTS

We are indebted to K. T. Waldeer for the initial version of the simulation code, and many helpful remarks during the study. We are grateful to R. Kelly for a critical reading of the manuscript and numerous helpful comments.

APPENDIX A

We present the solution of the collision-free Boltzmann equation

$$\frac{\partial f}{\partial t}+v_x\frac{\partial f}{\partial x}=0\ , \tag{A1}$$

with the boundary condition

$$f(x=0,\mathbf{v},t)=\frac{2}{\pi^3}e^{-\mathbf{v}^2/\pi}\Theta(v_x),\quad 0<t<1\ . \tag{A2}$$

Here we use scaled variables (cf. Sec. III B), but omit the tilde for brevity. The solution obviously reads

$$f(x,\mathbf{v},t)=\frac{2}{\pi^3}e^{-\mathbf{v}^2/\pi}\Theta(v_x),\quad 0<t-\frac{x}{v_x}<1\ , \tag{A3}$$

since every particle moves in a straight line with unchanged velocity.

Introducing the two velocities

$$\xi=\frac{x}{\sqrt{\pi}t},\quad \eta=\frac{x}{\sqrt{\pi}(t-1)}\ , \tag{A4}$$

the moments of the solution can readily be written down:

$$n(x,t)=\begin{cases}\operatorname{erfc}\xi, & t<1\\ \operatorname{erfc}\xi-\operatorname{erfc}\eta, & t>1\end{cases}$$
$$u(x,t)=\begin{cases}e^{-\xi^2}/\operatorname{erfc}\xi, & t<1\\ (e^{-\xi^2}-e^{-\eta^2})/(\operatorname{erfc}\xi-\operatorname{erfc}\eta), & t>1\end{cases} \tag{A5}$$

$$T_\parallel(x,t)=\begin{cases}1+\dfrac{2\xi e^{-\xi^2}}{\sqrt{\pi}\operatorname{erfc}\xi}-\dfrac{2e^{-2\xi^2}}{\pi\operatorname{erfc}^2\xi}, & t<1\\ 1+\dfrac{2}{\sqrt{\pi}}\dfrac{\xi e^{-\xi^2}-\eta e^{-\eta^2}}{\operatorname{erfc}\xi-\operatorname{erfc}\eta}-\dfrac{2}{\pi}\left[\dfrac{e^{-\xi^2}-e^{-\eta^2}}{\operatorname{erfc}\xi-\operatorname{erfc}\eta}\right]^2, & t>1\ .\end{cases}$$

Of course it is $T_\perp(x,t)\equiv 1$. We note that it is

$$n(x=0,t)=1\ ,\quad u(x=0,t)=1\ ,\quad T_\parallel(x=0,t)=1-\frac{2}{\pi} \tag{A6}$$

for $t<1$, and zero otherwise. Finally, the velocity distribution in the flow direction is given by

$$F(x,v_x,t)=\frac{2}{\pi}\begin{cases}\dfrac{e^{-v_x^2/\pi}}{\operatorname{erfc}\xi}\Theta(v_x)\Theta\left[t-\dfrac{x}{v_x}\right], & t<1\\ \dfrac{e^{-v_x^2/\pi}}{\operatorname{erfc}\xi-\operatorname{erfc}\eta}\Theta(v_x)\Theta\left[1-\dfrac{x}{v_x}-t\right]\Theta\left[t-\dfrac{x}{v_x}\right], & t>1\end{cases}, \tag{A7}$$

where Θ denotes Heaviside's step function. The velocity spectrum Eq. (24) is given by

$$J(v,\vartheta)=\frac{2}{\pi^2}v^3e^{-v^2/\pi}. \tag{A8}$$

Due to the absence of collisions, this result holds independently of the position of the detector x_D, and since this is a normalized distribution, it is independent of the flight angle ϑ.

APPENDIX B

We wish to present here the solution of the one-dimensional equations of ideal gas dynamics for a monoatomic gas,

$$\begin{aligned}&\frac{\partial n}{\partial t}+\frac{\partial}{\partial x}(nu)=0,\\ &n\frac{\partial u}{\partial t}+nu\frac{\partial u}{\partial x}=-c^2\frac{\partial n}{\partial x},\end{aligned} \tag{B1}$$

supplemented by the adiabatic equation of state

$$\frac{n}{n_K}=\left[\frac{c}{u_K}\right]^3. \tag{B2}$$

These equations are written in the conventional form with the exception that temperature has been expressed in terms of the adiabatic velocity of sound

$$c=\left[\frac{5}{3}\frac{1}{m}\frac{\partial p}{\partial n}\right]^{1/2}=\left[\frac{5}{3}\frac{kT}{m}\right]^{1/2}. \tag{B3}$$

The acceleration from the pressure gradient $-\partial p/\partial x$ has been rewritten correspondingly for adiabatic processes. Equations (B1) have to be solved for times $0<t<\tau$ with the boundary conditions

$$\begin{aligned}&u(x=0,t)=c(x=0,t)=u_K,\\ &n(x=0,t)=n_K,\\ &n(x\to\infty,t)=u(x\to\infty,t)=c(x\to\infty,t)\equiv 0,\end{aligned} \tag{B4}$$

with constant n_K,u_K. The first two of these boundary conditions have already been used in writing down the equation of state (B2).

Such expansion problems have been treated at length in Ref. 28. Since the problem at hand possesses no intrinsic length scale, the most convenient way to solve it is to look for a similarity solution in terms of the variable $\zeta=x/t$.[29] Then Eqs. (B1) read

$$\begin{aligned}&(u-\zeta)n'+nu'=0,\\ &\frac{c^2}{n}n'+(u-\zeta)u'=0,\end{aligned} \tag{B5}$$

where the prime denotes differentiation with respect to ζ. The system possesses a solution only if

$$u-\zeta=c, \tag{B6}$$

where waves traveling to the left ($u-\zeta=-c$) have been discarded. From Eq. (B5) we hence obtain

$$cn'+nu'=0, \tag{B7}$$

or

$$u=-\int c\frac{dn}{n}=-3\int dc=-3c+\text{const}, \tag{B8}$$

where we used the adiabatic equation of state (B2).

Equations (B5) and (B7) denote the solution to our problem. Introducing the boundary condition (B4), we finally obtain

$$\begin{aligned}&c(x,t)=u_K-\frac{1}{4}\frac{x}{t},\\ &u(x,t)=u_K+\frac{3}{4}\frac{x}{t}.\end{aligned} \tag{B9}$$

This solution is valid for $c\geq 0$, that is for

$$0\leq x\leq 4u_Kt. \tag{B10}$$

At the expansion front, the maximum velocity $u_{\max}$ is attained

$$u_{\max}=4u_K. \tag{B11}$$

[1]J. Cowin, D. Auerbach, and C. Becker, Surf. Sci. **78**, 545 (1978).
[2]I. Hussla, H. Coufal, F. Träger, and C. T. J. Chuang, J. Phys. **64**, 1070 (1986).
[3]W. Sesselman, E. E. Marinero, and T. J. Chuang, Appl. Phys. A **41**, 209 (1986).
[4]A. Namiki, T. Kawai, and K. Ichige, Surf. Sci. **166**, 562 (1986).
[5]R. Dreyfus, R. Kelly, and R. Walkup, Appl. Phys. Lett. **49**, 1478 (1986).
[6]A. Namiki, S. Cho, and K. Ichige, Jpn. J. Appl. Phys. **26**, 39 (1987).
[7]N. G. Utterback, S. P. Tang, and J. F. Friichtenicht, Phys. Fluids **19**, 900 (1976).
[8]R. Kelly and R. W. Dreyfus, Surf. Sci. **198**, 263 (1988).
[9]R. Kelly and R. W. Dreyfus, Nucl. Instrum. Methods B **32**, 341 (1988).

[10]R. Y. Kucherov and L. E. Rikenglaz, Zh. Eksp. Teor. Fiz. **37**, 125 (1959) [Sov. Phys.—JETP **37**, 88 (1960)].
[11]A. V. Luikov, T. L. Perelman, and S. I. Anisimov, Int. J. Heat Mass Transfer **14**, 177 (1971).
[12]S. I. Anisimov and Y. A. Imas, *Effects of High-Power Radiation on Metals* (National Technical Information Service, Springfield, VA, 1971).
[13]T. Ytrehus, in *Rarefied Gas Dynamics,* edited by J. L. Potter (Academic, New York, 1977), p. 1197.
[14]C. Cercignani, Commission of the European Communities Technical Report No. EUR 6843 EN, 1980 (unpublished).
[15]C. Cercignani, in *Rarefied Gas Dynamic,* edited by S. S. Fisher (American Institute of Aeronautics and Astronautics, New York, 1981), p. 305.
[16]A. Frezzotti, in *Rarefied Gas Dynamics,* edited by V. Boffi and C. Cercignani (Teubner, Stuttgart, 1986), Vol. 2, p. 313.
[17]G. A. Bird, *Molecular Gas Dynamics* (Clarendon, Oxford, 1976).
[18]M. Murakami and K. Oshima, in *Rarefied Gas Dynamics,* edited by M. Becker and M. Fiebig (Deutsche Forschungs- und Versuchsanstalt für Luft- und Raumfahrt Porz-Wann, 1974), Vol. 1, p. F.6-1.
[19]I. NoorBatcha, R. R. Lucchese, and Y. Zeiri, J. Chem. Phys. **86**, 5816 (1987).
[20]I. NoorBatcha, R. R. Lucchese, and Y. Zeiri, Phys. Rev. B **36**, 4978 (1987).
[21]L. Boltzmann, Ber. Wien. Akad. **66**, 275 (1872).
[22]C. Cercignani, *The Boltzmann Equation and Its Application* (Springer, Berlin, 1988).
[23]G. A. Bird, Phys. Fluids **13**, 2676 (1970).
[24]D. Sibold, Master's thesis, Technische Universität Braunschweig, 1989 (unpublished).
[25]D. Sibold and H. M. Urbassek (unpublished).
[26]R. Kelly (unpublished).
[27]I. NoorBatcha, R. R. Lucchese, and Y. Zeiri, Surf. Sci. **200**, 113 (1988).
[28]K. Stanyukovich, *Unsteady Motion of Continuous Media* (Pergamon, London, 1960).
[29]L. D. Landau and E. M. Lifshitz, *Fluid Mechanics,* Vol. VI of *Course of Theoretical Physics* (Pergamon, New York, 1959).